Neuron, Vol. 27, 635–646, September, 2000, Copyright ©2000 by Cell Press

Low Response Variability in Simultaneously Recorded Retinal, Thalamic, and Cortical Neurons

Prakash Kara, Pamela Reinagel, and R. Clay Reid*
Department of Neurobiology
Harvard Medical School
Boston, Massachusetts 02115

Summary

The response of a cortical cell to a repeated stimulus can be highly variable from one trial to the next. Much lower variability has been reported of retinal cells. We recorded visual responses simultaneously from three successive stages of the cat visual system: retinal ganglion cells (RGCs), thalamic (LGN) relay cells, and simple cells in layer 4 of primary visual cortex. Spike count variability was lower than that of a Poisson process at all three stages but increased at each stage. Absolute and relative refractory periods largely accounted for the reliability at all three stages. Our results show that cortical responses can be more reliable than previously thought. The differences in reliability in retina, LGN, and cortex can be explained by (1) decreasing firing rates and (2) decreasing absolute and relative refractory periods.

Introduction

The variability of evoked neural discharges is of central importance in the study of sensory systems. Reliable transmission of information depends not only on the average response to each different stimulus, but also on the variability of the response to any one stimulus. The discrimination of sensory stimuli is ultimately limited by the noise in neural responses. Neurons in the sensory periphery can have machine-like reliability (Rieke et al., 1997), whereas neurons in cortex often have highly variable responses (Shadlen and Newsome, 1998). It is tempting to assume that reliable sensory responses in the periphery acquire noise as a result of neural processing and become variable in cortex. This has only been a conjecture, however, as no one has ever demonstrated low variability in peripheral responses in an experiment also measuring high variability in cortical responses to the same stimulus. Thus, it has not been possible to exclude the alternative interpretation that differences between periphery and cortex were due to differences in stimuli or other experimental parameters.

When the same sensory stimulus is presented repeatedly, the number of evoked spikes will vary from trial to trial. In studies of the visual system, spike count variability is often quantified by the ratio of the variance to mean spike count, defined as the Fano factor (FF). This measure has a value of 1 if responses are as variable as a Poisson process, in which individual action potentials are generated at random times according to a time-varying firing rate.

*To whom correspondence should be addressed (e-mail: clay_reid@hms.harvard.edu).

Visual responses of retinal ganglion cells (RGCs) can be less variable than a Poisson process (FF $<$ 1) in isolated rabbit and salamander retinas (Berry et al., 1997). Low variability has also been reported in the retina of the anesthetized cat (Levine et al., 1992, 1996; Reich et al., 1997), in some cases using an indirect method of recording RGC activity from synaptic S potentials in the lateral geniculate nucleus (LGN). Thus, both in vitro and in vivo studies generally agree that RGCs can have low spike count variability under some conditions (but see Hartveit and Heggelund, 1994).

In mammals, RGCs project to relay cells in the LGN of the thalamus, which in turn project to visual cortex. Some studies have found high spike count variability (FF $>$ 1) in visual responses in the LGN of anesthetized cat (Sestokas and Lehmkuhle, 1988; Hartveit and Heggelund, 1994; Levine et al., 1996) and alert primate (Oram et al., 1999). However, in other studies, low spike count variability has been observed (FF $=$ 0.3–0.4) in the LGN of anesthetized cat (Reinagel and Reid, 2000) and alert monkey (Gur et al., 1997).

In visual cortex, variability has usually been computed from the number of spikes per cycle or "trial" of a periodic stimulus, typically 100–500 ms. Numerous studies in the visual cortex of anesthetized cat and anesthetized and alert monkey have found high variability of evoked responses (FF $=$ 1–3) (Heggelund and Albus, 1978; Dean, 1981; Tolhurst et al., 1983; Skottun et al., 1987; Vogels et al., 1989; Snowden et al., 1992; Swindale and Mitchell, 1994; Geisler and Albrecht, 1997; Bair and O'Keefe, 1998; Buračas et al., 1998; McAdams and Maunsell, 1999; Oram et al., 1999). To date, only two studies (both in the alert primate) have shown trial-by-trial variability (FF) of less than unity for a population of cells in a given cortical area. The first of these two studies showed that the variability in inferior temporal cortex (IT) (FF $=$ 0.82) was less than that in cortical area V1 (FF $=$ 1.18–1.43) (Gershon et al., 1998). In the second study (Gur et al., 1997), after selecting trials in which eye movements were negligible, V1 neurons had low variability (FF $\approx$ 0.4). Despite these counter-examples, the dogma persists that high variability is a fundamental characteristic of cortical responses, although it has been speculated that input layers with "privileged" connections may be an exception (Shadlen and Newsome, 1998).

The apparent differences in variability along successive stages in the visual pathway are difficult to interpret, however, because previous retinal, thalamic, and cortical studies have been done separately, often with different species, stimuli, and states of anesthesia. Thus, from the available literature, it is not possible to evaluate whether there is a dramatic increase in variability from retina to LGN to cortex or whether cortical variability could be as low as in retinal cells if the firing rates of cortical neurons were strongly modulated with effective stimuli.

To compare the trial-by-trial variability of visually evoked responses across different areas, we have made simultaneous single unit recordings from three successive stages of the cat visual system in vivo: (1) direct intraocular recording from RGCs, (2) from relay cells of the LGN, and (3) from simple cells in layer 4 of primary visual cortex, which receive direct synaptic input from

LGN relay cells. Visual responses were obtained using a drifting sine-grating stimulus. This experiment allowed us to compare variability of responses at all three levels under strictly identical conditions. In this study, we focus on the reliability (or variability) of spike count, but spike timing can also be highly reliable (e.g., Lankheet et al., 1989; Berry et al., 1997; de Ruyter van Steveninck et al., 1997; Reich et al., 1997; Reinagel and Reid, 2000).

We found that for simple cells in visual cortex, spike count variability was significantly lower than expected of a Poisson process. On average, the trial-by-trial variability doubled from retina to LGN and again from LGN to visual cortex. In some LGN cells, high variability was associated with bursting, which occurred at the onset of the visual response. Variability was inversely related to the overall mean firing rate in the three populations. Further, in individual cells at all three stages, variability decreased as firing rate increased within the stimulus cycle. A Poisson model with both absolute and relatively refractory properties largely accounted for the observed reliability of evoked responses, with the exception of the variability associated with LGN bursting. The increase in variability can therefore be ascribed to the decrease in the effects of refractoriness among neurons in the retina, LGN, and layer 4 of primary visual cortex.

Results

Variability of visually evoked responses was measured in a total of 54 neurons from nine animals (RGC, n = 17; LGN, n = 17; cortical simple cells, n = 20). The placement of electrodes in the three visual areas is illustrated in Figure 1A. Great care was taken to record only from well-isolated single units (Figures 1B and 1C), as described in the Experimental Procedures. In two LGN and two cortical recordings, a pair of well-isolated units were recorded on a single electrode (e.g., Figure 1B, LGN). Data were collected from (1) five simultaneous recordings from retina, LGN, and primary visual cortex (V1); (2) twelve simultaneous recordings from retina and visual cortex; and (3) ten recordings from LGN alone and one from striate cortex alone. In all of our simultaneous recordings, we identified a spatial frequency and orientation of the drifting sine grating that evoked strong responses from all cells.

Variability Is Low in Retina, LGN, and Cortex

We recorded from cells with overlapping receptive fields, for example, an off-center RGC, an off-center LGN relay cell, an on-center LGN relay cell, and a simple cell from striate cortex (Figure 2A). Our analysis was based on the simultaneous responses of the cells to a drifting sinusoidal grating (Figures 2B and 2C). The retinal and cortical cells' firing rate changed smoothly through the course of each stimulus cycle. By contrast, both LGN cells fired a burst of spikes at the onset of firing in nearly every stimulus cycle. These bursts resulted in a sharp transient peak in the peristimulus time histogram (PSTH) at the onset of the response. Other LGN cells that did not burst (n = 8/17) showed smooth variations in firing rate, similar to retinal and cortical cells.

Our first measure of trial-by-trial variability was the variance of the spike count in each 250 ms stimulus cycle divided by the mean (FF). For the example shown in Figure 2, the trial-by-trial variability was low in all three visual areas (RGC FF = 0.11, LGN FF = 0.20 and 0.24, and V1 FF = 0.33), compared with a Poisson process (FF = 1). Although variability was low, it increased at each successive recording site along the primary visual pathway.

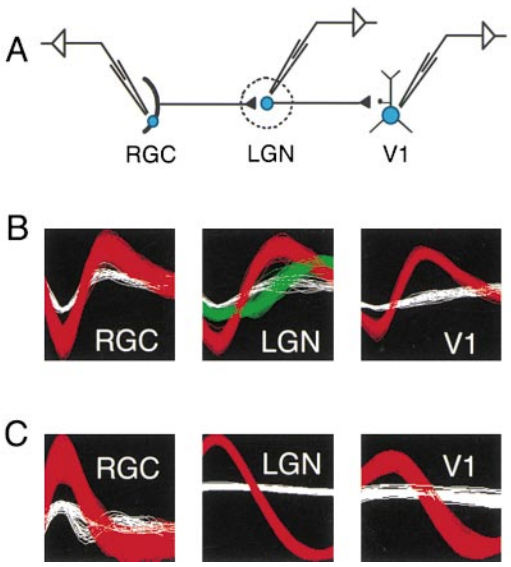

Figure 1. Simultaneous Spike Isolation in Retina, Thalamus, and Visual Cortex

(A) Schematic illustrating simultaneous recordings of an RGC, an LGN relay cell, and a layer 4 simple cell in primary visual cortex (V1).
(B) Action potential waveforms from an example simultaneous recording. The primary discriminated unit (action potential) on each electrode (RGC, LGN, V1) is shown in red. LGN electrode has a second discriminated unit (shown in green). Nondiscriminated units or background noise is shown in white. Several hundred action potentials are superimposed on each trace.
(C) Action potential waveforms from a simultaneous recording in a different animal.

The majority of our simultaneous recordings showed low variability in all cells, with a progressive increase in variability from retina through cortex (Figures 3A and 3B). RGCs had the lowest trial-by-trial variability (FF = 0.05–0.52). Variability in the LGN was somewhat higher (FF = 0.13–0.95). Cortical cells had the highest variability but were always less variable than a Poisson process (FF = 0.28–0.94). Two LGN cells with uncommonly high variability (FF = 0.87 and 0.95) were a simultaneously recorded pair (open symbols in Figure 3A). These cells had receptive field properties and bursting frequencies typical of the population. The only unusual feature we noted was a high level of background firing by the LGN cell with the higher variability.

We pooled the data from all recordings to calculate the mean trial-by-trial variability for retinal, thalamic, and cortical cell populations (Figure 3C). The average variability significantly increased (approximately doubled) from retina to thalamus (mean FF = 0.15 versus 0.32, $p < 0.005$, Mann-Whitney [MW] test) and from thalamus to cortex (FF = 0.32 versus 0.55, $p < 0.0005$, MW test). We also found that the mean firing rate significantly decreased from retina to LGN (from 36 to 18 spikes/s, $p < 0.005$, MW test) and from LGN to cortex (18 to 8 spikes/s, $p < 0.001$, MW test), suggesting a general relationship between firing rate and reliability (Figure 3D). We investigated the dependence of firing rate on

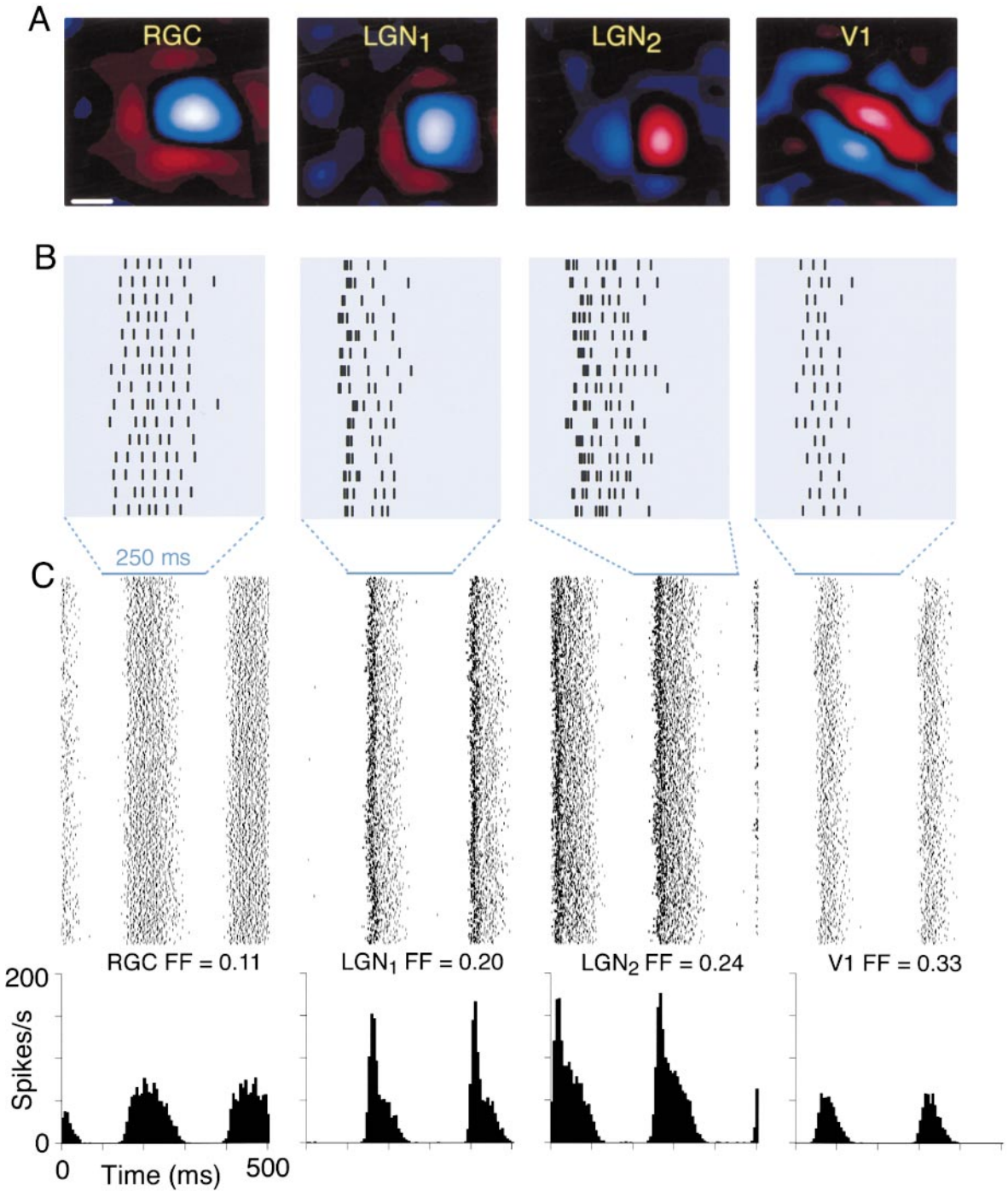

Figure 2. Simultaneous Recording from Retina, Thalamus, and Visual Cortex

(A) Receptive field maps of an off-center RGC, an off- and an on-center LGN cell, and a simple cell from striate cortex recorded simultaneously. Spike waveforms of these cells are shown in Figure 1B. Receptive fields centers from the various sites were overlapped to within 1°. Color codes for response sign (red for *on* responses and blue for *off* responses), and brightness codes for response strength. Scale bar, 1 pixel (0.8°).

(B) Responses of cells shown in (A) to a drifting sine-grating stimulus. Each vertical line on the raster plot represents an action potential. Each row represents the response to one cycle of the periodic stimulus. Only 15 of the 800 cycles are represented. Both LGN responses have bursts of spikes at the onset of firing in each cycle. Such bursts were absent in retinal and cortical recordings.

(C) Raster plots as in (B), but showing responses to all 800 cycles (400 samples of two stimulus cycles), with each spike represented by a dot. Responses for the two LGN cells are out of phase from each other because of the opposite sign of their receptive field centers. Beneath the rasters are the PSTHs of the same data. The variability of the spike count in single cycles of the visual stimulus (250 ms) is given by the FF.

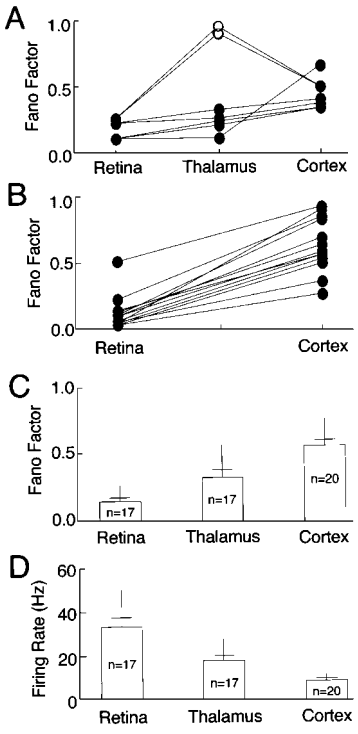

Figure 3. Variability of Spike Count in One Stimulus Cycle

(A) Variability (Fano factor [FF]) of responses from simultaneous recordings in retina, thalamus, and cortex. Symbols connected by lines represent cells that were recorded simultaneously. Spikes were counted in a 250 ms window, comprising one cycle of the sinusoidal stimulus. With the exception of two thalamic (LGN) cells (open symbols), variability at all three recording sites was much lower than that of a Poisson process (FF $<$ 1).

(B) FF of responses from simultaneous recordings in retina and cortex, analyzed as in (A). Retinal cells were less variable than were simultaneously recorded V1 neurons.

(C) FF significantly increased (approximately doubled) from retina to thalamus ($p < 0.005$) and from thalamus to visual cortex ($p < 0.0005$). Vertical error lines represent standard deviations, and smaller horizontal error lines represent standard errors of the mean.

(D) The overall mean firing rate in spikes/s (Hz) significantly decreased by ~2-fold from retina to thalamus ($p < 0.005$) and from thalamus to cortex ($p < 0.001$). Error bars as in (C).

variability further by exploring whether variability changes within the course of a stimulus cycle in the responses of individual cells.

Variability Is Anticorrelated with Firing Rate

Previous studies have observed that retinal cells fire more regularly as their firing rate increases (Rodieck, 1967; Barlow and Levick, 1969; Frishman and Levine, 1983). In our experiments, we used a drifting sinusoidal grating stimulus, and the firing rate of each cell was modulated through the course of the stimulus cycle (Figure 2C). We therefore tested the dependence of reliability on firing rate by examining how the FF changed over time within a trial as firing rate varied between zero and maximum firing.

We calculated the FF in a 50 ms sliding window (see Experimental Procedures). The mean spike count in this window represents a smoothed version of the PSTH (Figure 4A). If the variance were proportional to the mean count, as for a rate-modulated Poisson process, the FF would be constant throughout the cycle. Instead, we found that the FF varied throughout the trial (Figure 4B).

For the retinal and cortical cells shown, the variability was lowest when the firing rate was highest, and vice versa. Specifically, in the RGC, the mean spike count changed gradually from 0 spikes to 3.4 spikes/50 ms window (68 spikes/s), and the variability (FF) reached a minimum of 0.08 during times of maximum firing. Similarly, the cortical response reached a minimum FF of 0.23 in the time bin with the highest firing rate (mean count, 2.4, or 48 spikes/s). LGN responses sometimes deviated from such a smooth relationship between firing rate and variability.

For the two LGN cells shown, the onset of firing in each cycle coincided with very high, supra-Poisson variability (peak FF = 1.73 and 2.07; Figures 4A and 4B). This peak in variability at response onset was found only for LGN cells that fired bursts. Thalamic relay neurons fire bursts of spikes due to low-threshold calcium spikes (Jahnsen and Llinás, 1984; Steriade and Llinás, 1988; McCormick and Feeser, 1990). These bursts are unitary firing events that can be stimulus evoked (Sherman, 1996; Reinagel et al., 1999). If we retained only the first spike of each burst in our analysis (see Experimental Procedures), the variability was sub-Poisson at all times in the trial. FF then varied inversely with firing rate, as found for retinal, cortical, and nonbursting LGN cells (data not shown).

We considered three specific ways that bursts could have caused high variability: (1) the stimulus evoked a burst in some trials, but single spikes in other trials, (2) the number of spikes within the burst was variable from trial to trial, and (3) the bursts occurred at different times in each trial. The two LGN responses shown in Figure 4 had a single burst at the onset of nearly every stimulus cycle (92% and 89% of cycles). The numbers of spikes in the identified bursts were also reliable (spikes per burst: 2.53 $\pm$ 0.6 for LGN_1 and 2.56 $\pm$ 0.7 for LGN_2, mean $\pm$ SD). To test whether variable timing caused the high variability, we aligned the responses by the first spike in each cycle. The first 50 ms of the aligned LGN response included the entire burst on each trial and had sub-Poisson spike count variability for the two LGN cells shown (FF = 0.14 and 0.16). Thus, response variability at the onset of the LGN response was primarily due to the variable onset time of the burst. Despite this complication at the onset of firing, later in the trial these LGN responses followed the same trend as retinal and cortical responses did. Variability decreased as firing rate increased to its maximum (90 and 116 spikes/s) for a minimum FF of 0.15 and 0.16 in the two LGN cells.

Thus, in general variability was inversely related to firing rate in individual neurons' responses. In the previous section, we showed that the mean firing rate per stimulus cycle decreased from retina to LGN to cortex, while average variability increased from one stage to the next (Figure 3). To test if these differences in firing rate were sufficient to account for the differences in variability, we compared the variability of responses as a function of firing rate (spike count). For each population of cells, we compared the variance in spike count to the mean spike count in overlapping 50 ms windows throughout the stimulus cycle (Figure 4C). In all three populations of cells, many 50 ms windows had variance well below the mean count, and therefore FF $<$ 1. RGC responses approached the minimum possible variance

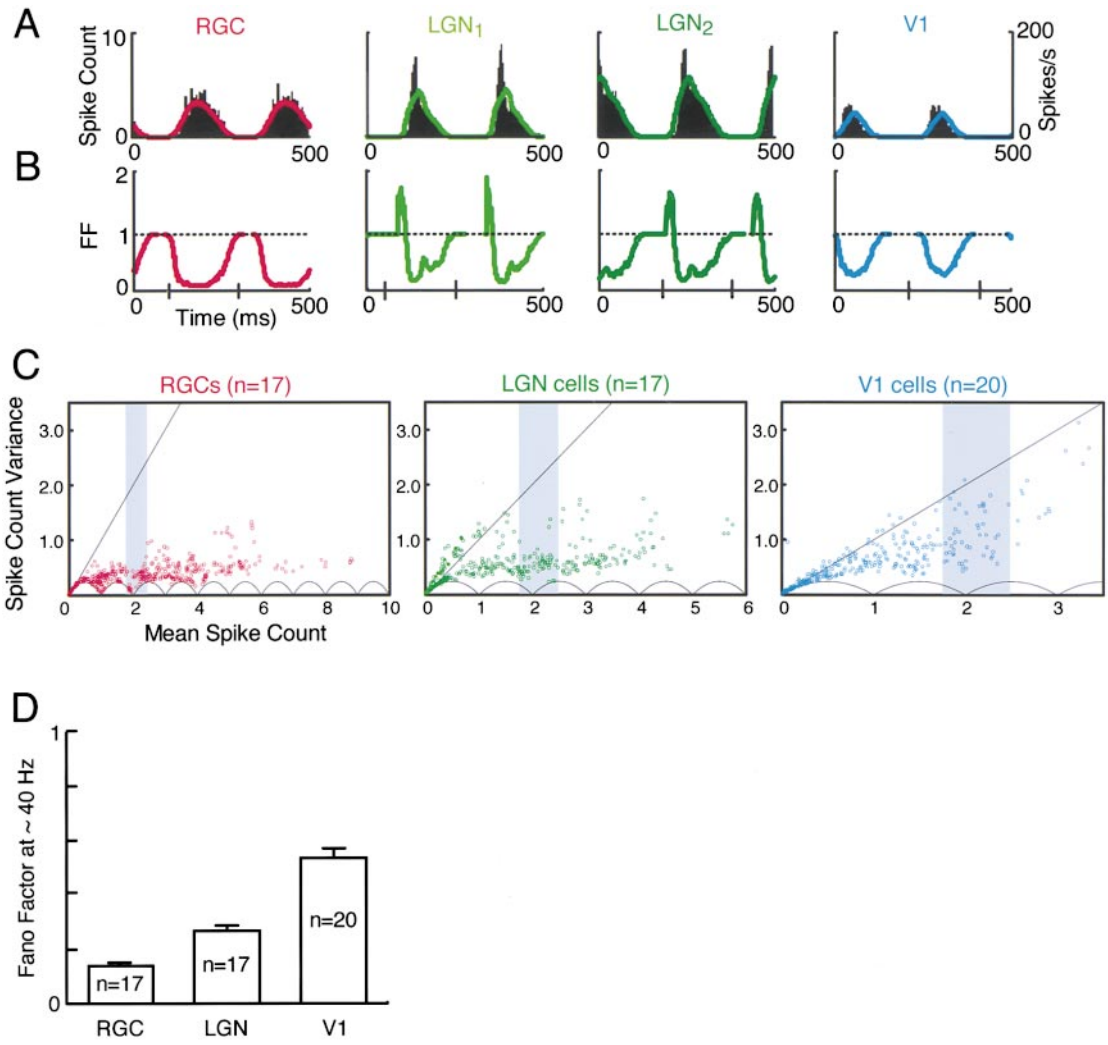

Figure 4. Variability Depends on Firing Rate through the Course of the Stimulus Cycle

(A) Mean spike count (firing rate) in a sliding 50 ms counting window for retinal (red trace), LGN (green traces), and cortical (blue trace) data. Each point on this curve plots the spike count in a 50 ms window versus the time of the center of that counting window. Data are from the same four cells shown in Figure 2. For comparison, black histograms show PSTH using 3 ms bins scaled to the same units on all four plots (spikes/50 ms window on left axis or firing rate in spikes/s on right axis).

(B) Fano factor (FF) through the course of a stimulus cycle. Time axis, same as in (A). FF was lowest at the peak of the evoked response of each cell. Both LGN cells showed high variability at response onset, as was found for all LGN cells that fired bursts. Tick marks on the time axis indicate the start and stop of the portion of the data shown in Figures 5A, 5B, and 6A.

(C) Mean spike count versus variance for all cells in the population. Each point represents the mean and variance of the spike count in a given 50 ms window at a fixed time, t, relative to the stimulus cycle, computed from 200 samples from a single cell. Results are shown for sliding 50 ms counting windows that overlapped by 25 ms. Retinal data shown in red, LGN in green, cortical data in blue. The first 50 ms window of the visual response of bursting LGN cells is shown in closed green symbols. Data for a Poisson process would fall on the line of mean = variance (FF = 1), diagonal line. The minimum possible variance (from integer spike counts) is shown by the scalloped curve. The shaded area shows the range of spike counts (1.8 to 2.4 spikes) analyzed in (D).

(D) FF increases from retina to cortex even when firing rate is matched. Each bar shows the average FF over all cells in the population, in sample windows that had spike counts between 1.8 and 2.4 spikes (firing rate, ~40 spikes/s). Error bars show standard error of the mean.

(scalloped curve, see Figure 4 legend) over a wide range of mean counts (firing rates). Responses of LGN neurons sometimes had variance exceeding the mean (and therefore FF $>$ 1), in many cases attributable to bursting (closed symbols). Nonetheless, samples from other phases of the response and from other LGN cells had variance closer to the minimum than the mean. Typically, cortical responses also had variances less than the mean but higher than the theoretical minimum.

At a given mean count (e.g., shaded area in Figure 4C), retinal data were less variable on average than LGN, and LGN less variable than cortex. For example, we averaged the FF of all 50 ms windows that had a mean spike count between 1.8 and 2.4 spikes (firing rate of ~40 spikes/s; Figure 4D). Even when firing rate was the same, variability significantly increased from retina (FF = 0.14) to LGN (FF = 0.27) to cortex (FF = 0.54) ($p < 0.0001$, Kruskal Wallis; Mann-Whitney comparisons, $p <$

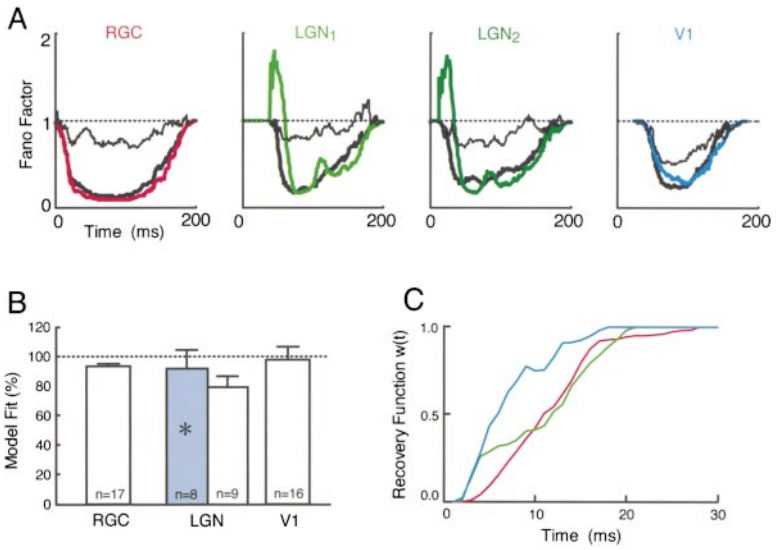

Figure 5. Fano Factor throughout the Trial in Model Responses

(A) Fano factor (FF) in 50 ms windows during the visual response of each cell, where the time axis is shifted in phase and expanded from between the tick marks on the time axis of Figure 4B (red, green, and blue traces). Dashed line indicates FF = 1, the variability of any Poisson process in any counting window. Thin black curves represent FF of models that matched the time-varying rate (PSTH) and also the estimated absolute refractory period of each neuron. Thick black curves represent FF of Poisson models that matched the PSTH and the estimated absolute and relative refractory periods of the neurons. For details of both models, see Experimental Procedures.

(B) Quality of the fit of the model with a relative refractory period, as judged from comparing the model FF to the data FF at the time in the cycle when data variability was lowest (minima of colored lines in [A]). Fit is defined as 100 × (1 − model)/(1 − data). A perfect fit has a value of 100%, and values less than this indicate that the spike count of the model cell was not as reliable as the data. All populations had a fit of 80% or better. Retinal results based on n = 17 cells. Cortical results based on n = 16 cells; the remaining four cortical cells had too few spikes for the estimation of the refractory period (see Experimental Procedures). LGN cells that did not fire bursts were modeled exactly as retinal and cortical cells (open bar, n = 9). For LGN cells with bursts, estimation of the refractory period was based on data in the nonbursting part of the stimulus cycle, if any existed (gray bar, n = 7). If refractory periods were estimated instead from a mixture of burst and nonburst interspike intervals, the resulting model fit poorly (asterisk, n = 8). Error bars show standard error of the mean.

(C) Recovery functions from the models, w(t), averaged over all retinal (red), LGN (green), or cortical (blue) cells. The duration of the estimated relative refractory period decreased at successive stages of the visual pathway. For bursting LGN neurons, these recovery functions were fit to the nonburst epochs of the responses.

0.0001). Therefore, firing rate alone did not predict variability.

Refractory Periods Account for Neural Reliability

Refractory periods are expected to make neural responses more regular, particularly when firing rate is high (Teich et al., 1978; Teich and Diament, 1980; Berry and Meister, 1998; Barberini et al., 2000). We therefore tested whether refractoriness could account for the high reliability in our data. First, we modeled the response of each cell by a Poisson process modified to enforce a dead time following each spike. Each model was determined by the observed time-varying firing rate and the estimated absolute refractory period of the neuron and therefore had no free parameters (see Experimental Procedures). Unlike a pure Poisson process (FF = 1 in all counting windows), the model with an absolute refractory period had lower variability at times in the trial when firing rate was high (thin black lines in Figure 5A). The model nevertheless had dramatically higher variability than the real data from retina, LGN, and cortex (red, green, and blue lines in Figure 5A).

Our second model incorporated both an absolute refractory period and a longer relative refractory period (Teich and Diament, 1980; Berry and Meister, 1998). The rate of the underlying Poisson process was uniquely determined by the constraint of matching the observed firing rate of the neuron. The time course of recovery of spiking after each action potential was estimated from the observed interspike interval distribution (see Experimental Procedures). Thus, this model also had no free parameters. The model with a relative refractory period was much better at matching the time-varying FF of both retinal and cortical cells (thick black lines in Figure 5A).

One measure of the quality of the model is its ability to account for the least variable part of each cell's response (compare the minima of the red, green, and blue lines with the thick line at the same time point, Figure 5A). We expressed the fit of this model as 100 × (1 − FF_{model})/(1 − FF_{data}) (%). The discrepancy between the model and the data was <10% for RGCs, <20% for both bursting and nonbursting LGN cells, and <5% for cortical cells (Figure 5B). Thus, refractoriness accounted for much of the observed reliability of our data.

The model of each cell was based on its estimated recovery following a spike (see Experimental Procedures). This recovery function was slowest for retinal cells and fastest for cortical cells (Figure 5C). The recovery function of LGN neurons often appeared to have two components. These two components were seen for most but not all individual LGN neurons. We note that the absolute and relative refractory periods of the model could reflect any form of refractoriness, not only that arising from the active conductances of the neuron. For example, refractoriness in synaptic transmission could also contribute to the refractoriness observed at the level of spiking statistics.

The one aspect of the data not fit by the model was the high variability associated with LGN bursts. This is not surprising, since adding refractoriness to any model only increases its regularity, whereas this part of the LGN response was already more variable than the Poisson starting model. For bursting LGN cells, we used the nonbursty part of the response in each cycle to estimate the refractory period and then used this refractory period to model the entire response (see Experimental Procedures).

Variability Is Sub-Poisson for Counting Window Lengths from 1 to 1000 ms

In general, the FF depends on the size of the window in which spikes are counted (T) (Thurner et al., 1997). In

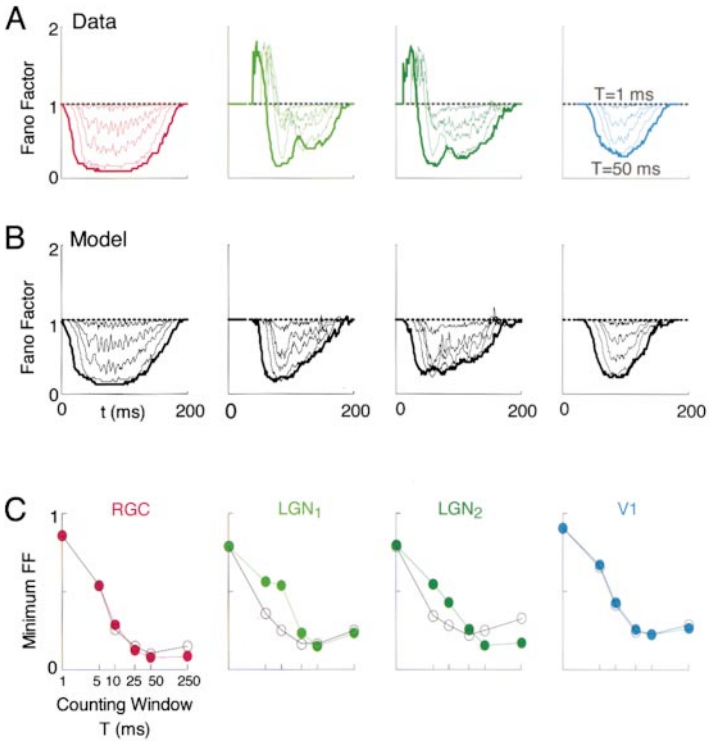

Figure 6. Fano Factor Depends on the Size of Counting Window

(A) FF(T,t) through the visual response, computed in counting windows T = 1, 5, 10, 25, and 50 ms. Dotted line indicates Fano factor (FF) = 1. Thick curve shows results for T = 50 ms (as in Figure 5A). In each panel, the uppermost thin curve in the sub-Poisson regime shows results for T = 1 ms, and lower curves correspond to progressively larger counting windows. As in Figure 5A, each point plots the FF in window of length T versus the time of the center of the counting window. Over this range of small counting windows, FF was <1 in all epochs of retinal and cortical responses and in the nonburst portion of LGN responses. Note that the epoch of high variability in the LGN is associated with burst onset, and the time (t) of the first counting window to capture burst onset is necessarily later for smaller windows.

(B) FF(T,t) of model with relative refractory period for each cell, plotted as in (A). The model qualitatively reproduced the dependence of FF on counting window T.

(C) Minima of FF(t) for data and models shown in (A) and (B) at each counting window size (T). Data shown in closed color circles, models shown as open circles. At the shortest counting window (T = 1 ms), the minimum FF is close to unity. With larger counting windows (T = 5 to 250), the minimum FF progressively decreases. For retinal ganglion (red) and cortical (blue) cells, model closely matched data at all counting windows. For LGN cells containing bursts (green), model deviated from data for some counting windows (see text).

our experiments, we found FF to change as a function of both counting window, T, and time within the stimulus cycle, t (Figure 6A). In very small counting windows (1 ms), FF was near 1 at all times throughout the stimulus cycle. This result is expected from any model, because the mean spike count in any 1 ms window is small, and the count in any individual window can only be 0 or 1. The modulation of FF through the stimulus cycle emerged and progressively increased as the counting window increased up to T = 50 ms, such that spike counts were high enough to observe the regularity of the responses.

The model with both absolute and relative refractory periods reproduced the detailed dependence of FF(t) on the counting window size T, other than the effects of LGN bursts (Figure 6B). For the retinal cell shown in Figure 6A, the small oscillations in FF were also reproduced by the model (Figure 6B). These reflect oscillatory peaks in firing rate that were phase locked to the refresh rate of the video stimulus (not evident at the temporal resolution shown in Figure 2C). We found no significant correlation between the FF and the presence of such phase-locked peaks. In fact, the lowest FF in our sample (FF = 0.05) was for a retinal cell that completely lacked such oscillatory peaks.

To summarize the effect of the counting window on our estimates, we compared the minimum FF for a range of counting windows (closed symbols in Figure 6C). The minimum FF decreased as the size of the counting window increased from 1 to 50 ms. This trend is reproduced by the model (open symbols in Figure 6C). For comparison, we also show the minimum FF in a full stimulus cycle (T = 250).

Two previous cortical studies reported FF as a function of T, either for T = 1 to 1000 ms (Buračas et al., 1998) or for T = 0.001 to 770 s (Teich et al., 1996). Both studies found that FF was greater than unity and increased with T over the range explored. Therefore, although we obtained FF < 1 in small counting windows, we considered the possibility that our cortical cells might have supra-Poisson FFs in larger counting windows. When we used T = 1 s (four stimulus cycles), we still obtained sub-Poisson variability in our populations of cells: FF = 0.26 ± 0.07 (mean ± SEM) for RGCs (n = 17), FF = 0.37 ± 0.08 for LGN (n = 17), and FF = 0.68 ± 0.07 for V1 (n = 19). For most cells, we analyzed only 200 s of data and counting windows up to 1 s. In general, we therefore cannot exclude the possibility that we might have found FF > 1 if we had considered much longer recording times or used longer counting windows. In the few cases in which we had very long recordings (up to 50 min), however, the variability over the entire data set at T = 250 ms was sub-Poisson, as was the FF in counting windows of up to T = 8 s (data not shown).

Although FF depended on the size of the counting window, our main conclusions held over a wide range of windows: (1) FF was <1 for all three cell types; (2) FF was lowest in retina, intermediate in LGN, and highest in cortex; and (3) a Poisson model with a relative refractory period reproduced the FF throughout the stimulus cycle, except for LGN bursts.

Discussion

We have shown that trial-by-trial response variability of cortical cells can be much lower than previously believed. We recorded from 20 simple cells in layer 4 of

primary visual cortex during visual stimulation and found low variability was the rule rather than the exception. Regardless of the size of the counting window (up to 1 s), we found that the FF was below 1 for all cells in this sample. We have demonstrated that variability is lower in the LGN than in cortex, and lower still in RGCs. Thus, neural responses became more variable as they traversed these synaptic levels. By recording simultaneously at multiple levels of the visual system, we have been able to show that this increase can be found in individual animals under literally identical visual stimulation and physiological conditions. We have shown that Poisson models modified with relative and absolute refractory periods can account for most aspects of neural reliability in all three cell populations. The only major feature of the data not captured by the model was the variability associated with LGN bursting.

Sub-Poisson Variability in Cortex

Our finding of low variability in cortical neurons goes against the general belief that cortical neurons are always noisy (Softky and Koch, 1993; Ferster, 1996; deCharms and Zador, 2000). The main difference between our study and previous studies in cortex is that we have specifically targeted layer 4 simple cells in primary visual cortex, whereas most other studies have recorded from all cortical layers. Thus, we have selected a population of cells that receives direct monosynaptic input from relay cells of the LGN. In layer 4, thalamocortical synapses onto layer 4 neurons are both stronger and more reliable than synapses from intracortical neurons (Tanaka, 1983; Reid and Alonso, 1995; Alonso et al., 1996; Stratford et al., 1996). Therefore, it is possible that layer 4 simple cells have much lower variability than cells in other layers or cortical areas, as had been previously postulated (Shadlen and Newsome, 1998). Two previous studies have reported low variability in a population of cortical neurons. One study reported low variability in responses of V1 neurons in alert monkeys after trials with eye movements were excluded from analysis (Gur et al., 1997). Interestingly, most of the cells in that study were also recorded in layer 4. The second study reported high variability in layer 2/3 of V1, with somewhat lower variability in unidentified layers in IT (Gershon et al., 1998).

Some previous cortical studies may have also differed from ours in the effectiveness of the stimulus, which can affect response variability. In four cortical cells, we calculated variability of responses to each of 16 different orientations of a drifting sinusoidal grating. We found that for any given cell, variability was lowest (sub-Poisson) for the grating that drove the cell best and higher for less effective orientations, reaching FF $>$ 1 for some orientations (data not shown). When two cortical cells with different orientation preferences were recorded simultaneously, a single orientation produced high variability in one unit at the same time that it produced low variability in the other. We interpret the dependence on the stimulus as arising from the greater effects of refractoriness when firing rate is high. Berry et al. (1997) provided the same explanation as to why RGCs had reliable responses to high-contrast stimuli and more variable responses to lower contrast visual stimuli. Nonetheless, at least some previous cortical studies have found high variability even when average firing rates were high (e.g., Tolhurst et al., 1983; Buračas et al., 1998; Shadlen and Newsome, 1998; Barberini et al., 2000). Therefore, previous findings of much higher variability in cortex cannot generally be explained by stimulus differences.

One study of eight cells from the medial temporal area (area MT) in monkeys reported Poisson variability (FF $\approx$ 1) in 100 ms counting windows but low variability (FF $\approx$ 0.6) in 10 ms counting windows (Barberini et al., 2000). By comparison, our cortical responses had sub-Poisson variability in both short and long counting windows (up to at least 1000 ms). Although FF depends on the size of the counting window, we do not think this is the reason our results differ from previous cortical studies, as we found FF $<$ 1 for counting windows ranging from 5 to 1000 ms, covering the range of windows used in nearly all previous studies that found FF $>$ 1 in cortex.

Our study also differs from many others in that we used a longer (200 s) continuous recording time with a given visual stimulus. This provided many samples (n = 200–800) for estimation of the mean and variance of the spike count. In addition, any effects of adaptation to the stimulus would occur in the first few seconds and affect only a small fraction of the samples. Some previous studies may have obtained high variability because estimates were based on few samples or because samples were taken from short, interleaved trials in which cells never attained a steady-state response.

Finally, variability in neural responses could be introduced by any source of experimental variability, such as fluctuations in anesthesia (Kisley and Gerstein, 1999), small eye movements in alert animals (Gur et al., 1997), and neuromodulators (Hartveit and Heggelund, 1994; Kara and Friedlander, 1999). Such stimulus-independent variables would be expected to affect the reliability of responses as early as the LGN. Simultaneous recordings with low variability in the LGN could therefore serve as a useful internal control against many of these factors in future studies of cortical variability.

Of all the factors considered above, the most consistent difference between our experiment and previous studies is that we recorded only from cells that receive strong feedforward input from the thalamus, namely, layer 4 simple cells of primary visual cortex.

Variability Increases from Periphery to Cortex

We found that variability increased from retina to LGN to cortex in simultaneous recordings (Figures 3A and 3B) and on average over the population (Figure 3C). Comparing the three populations of cells, average variability (FF) was inversely related to mean firing rate (Figures 3C and 3D). The different mean rates, however, did not account for all differences in variability. Even when we compared epochs of the response with the same firing rate, we found that variability increased from retina through cortex (Figures 4C and 4D). We attribute this to differences in refractoriness (see below).

Our finding of low variability in RGCs is consistent with most previous reports. For the LGN, the low variability we found with gratings is comparable to that reported for responses to full-field white-noise stimuli in anesthetized cat (Reinagel and Reid, 2000). Low variability was also reported in the LGN of alert primate, when trials with eye movements were excluded (Gur et al., 1997). In several other studies, supra-Poisson variability was found in LGN responses (Sestokas and Lehmkuhle,

1988; Hartveit and Heggelund, 1994; Oram et al., 1999). In these studies, stimuli were flashed in the center of the LGN receptive field, whereas all studies (including ours) that found low variability used moving or dynamic stimuli that extended far outside the receptive field centers. It would be interesting therefore to explicitly test the effects of these stimulus parameters on variability for a given cell.

Bursts in the LGN

Some LGN cells fired bursts at the onset of firing and exhibited high spike count variability through part of the stimulus cycle. We found that this was primarily due to variability in the time of the burst from trial to trial, rather than variability in the occurrence of the burst or the number of spikes in the burst. However, this is not to say that bursts were any more variable than other spikes in their timing. Our results are consistent with previous findings that the timing of LGN bursts is reliable (Guido and Sherman, 1998). We attribute the high spike count variability to the abrupt change in firing rate, from 0 spikes/s before the burst to >200 spikes/s within the burst. In small counting windows early in the response, some trials contain the burst (and thus many spikes), while other trials do not (no spikes), leading to a variance much higher than the mean count. The transition from the burst to a moderate firing rate afterward is less abrupt, giving rise to a small but detectable second peak in variability (Figure 4A). Bursting did not affect our measure of variability in 250 ms counting windows, because the counting window included the entire burst in every trial, regardless of its exact timing.

Refractoriness Can Account for Reliability

Poisson model spike trains incorporating relative and absolute refractory periods accounted for the most reliable part of the response, with models differing from data by 5%–20% in all three types of cells (Figure 5B). It was previously shown that the same model could largely account for the reliability of spike count in RGCs of the salamander (Berry and Meister, 1998). In that study, ganglion cells were also slightly more reliable than predicted by the model. Our results replicate their finding for the retina and extend it to LGN and cortex.

Spiking statistics can also be captured in a mathematically simpler model, at the expense of biophysical realism. For example, a gamma model of order N is obtained by taking every Nth spike of a Poisson process (see Experimental Procedures). Such a model depends only on the time-varying firing rate and a single free parameter, the order. Gamma models have some properties in common with refractory cells, including low spike count variability (Stein, 1965). We found that a gamma model of sufficient order (generally 3–6) could also match FF as a function of counting window (T) and time in the cycle (t) about as well as an explicit refractory model could (data not shown). We did not explore gamma models of time-varying order (but see Gazères et al., 1998).

We have suggested that differences in refractoriness could explain the fact that even in epochs of similar firing rate, variability increased from retina to cortex (Figure 4D). In agreement with this interpretation, the duration of the estimated relative refractory periods was longer for RGCs, intermediate for LGN cells, and shortest for cortical cells (Figure 5C). If the refractory period itself depends on firing rate, the difference we found between retina, LGN, and cortex could be an indirect effect of their different long-term activity. Indeed, increasing levels of maintained discharge in the retina (Barlow and Levick, 1969) led to estimated refractory periods of increasing duration (Teich et al., 1978). However, we were not able to demonstrate any dependence on firing rate on short time scales; refractory periods estimated from different phases of the stimulus cycle were indistinguishable (data not shown).

We found that a model with only an absolute refractory period was inadequate to match the reliability in our data (Figure 5A). The inadequacy of this "dead time" model was much more pronounced for retinal cells than for cortical cells. Barberini et al. (2000) also explored dead time models to explain the sub-Poisson variability in their MT data when they used 10 ms counting windows. They report that the MT data were only moderately less variable than a dead time modified Poisson process, whereas data from fly H1 neurons were dramatically less variable than a dead time model. These dead time models took into account that H1 neurons have longer absolute refractory periods than monkey MT neurons do. Thus, the authors concluded that differences in reliability between MT and H1 were not explained by differences in refractoriness. The results just summarized from MT and H1 are qualitatively similar to our results from dead time models in cortical cells and RGCs, respectively. We found that a more complete model of refractoriness, with a relative as well as absolute refractory period, could fit both retinal and cortical responses comparably (Figure 5B). Therefore, we think that differences in the duration of both absolute and relative refractory periods can explain the differences between our cell populations and could potentially explain the differences between MT and H1, as well. An extreme hypothesis would be that cortical cells are no more "noisy" than retinal cells are, once refractoriness is taken into account. A complementary way to put this is that retinal cells are just as noisy as cortical cells, before their responses are regularized by refractoriness. Thus, the noise introduced by neural processing could be just as great in the retina as in cortex.

In conclusion, at least one class of cortical cells (layer 4 simple cells in striate cortex) can exhibit low, sub-Poisson spike count variability. Along the first few stages of the primary visual pathway, variability increased at each processing stage. The simplest explanation of our data is that the reliability of spike count is a consequence of the refractory properties of neurons. Simultaneous measurement of variability across ascending levels in the visual hierarchy will continue to be useful in future studies of the origins and extent of neural variability.

Experimental Procedures

Preparation and Anesthesia

Experiments were performed on nine anesthetized, paralyzed adult cats (2.5–3.5 kg). Animals received dexamethasone (~1 mg/kg, i.m.) 12–14 hr before surgery and again at time of surgery along with atropine sulfate (0.1 mg/kg, subcutaneous). Anesthesia was induced with ketamine HCl (10 mg/kg, i.m.) and maintained with thiopental sodium (20 mg/kg, i.v., supplemented as needed). All pressure points and incision sites were treated with a topical anesthetic (2% lidocaine HCl). A tracheotomy was performed and the animal transferred to a Horsley-Clarke stereotaxic frame. Body temperature (38°C), electrocardiogram, and expired CO_2 were monitored continuously and maintained within normal limits. The electroencephalogram over the frontal lobes was monitored to assess anesthesia.

Pupils were dilated with 1% atropine sulfate and nictitating membranes retracted with 10% phenylephrine. Craniotomies were made over the left hemisphere of the brain corresponding to LGN and primary visual cortex (area 17). A metal ring was glued to surgically exposed lateral sclera of the right (contralateral) eye and attached to a post to prevent small eye drifts that may otherwise occur even with adequate anesthesia and paralysis. The metal ring also facilitated the insertion of an intraocular recording electrode (see below). A fiberoptic light source was used to reflect retinal landmarks onto a tangent screen placed 114 cm in front of the eyes (Pettigrew et al., 1979). Optical refraction was achieved with gas-permeable contact lenses (+2.0 to +4.0 diopters) such that surface retinal blood vessels were focused on the tangent screen.

After all surgical procedures were complete, anesthesia was maintained with thiopental sodium (2–3 mg/kg/hr, in 0.9% saline, i.v.). Paralysis was achieved by vecuronium bromide (0.2–0.3 mg/kg/hr, in 0.9% saline with 5% dextrose, i.v.). Animals were mechanically ventilated, and expired CO_2 was regulated at 3.8%–4.2%. All surgical and experimental procedures were in accordance with National Institutes of Health and United States Department of Agriculture guidelines and were approved by the Harvard Medical Area Standing Committee on Animals.

Electrophysiology, Visual Stimulation, and Receptive Fields

Simultaneous recordings from RGCs, LGN cells, and simple cells in striate cortex were made with platinum-plated tungsten-in-glass electrodes (Merrill and Ainsworth, 1972). Electrodes in each area were positioned so that receptive field centers across all three areas shared similar eccentricity (~2°–5° from area centralis) and were completely or partially overlapped with one another (within 2° of visual angle). Similar procedures were used in experiments with only two electrodes (retina and cortex) or one electrode (LGN or cortex).

Typically, a recording session began with retinotopic mapping of the A laminae of the dorsal LGN (Sanderson, 1971a, 1971b). We avoided recording from the medial interlaminar nucleus by the methods of Malpeli (Lee et al., 1984, 1992). After the retinotopy of the LGN was mapped, we searched for simple cells along the medial bank of the striate cortex. We recorded from simple cells with at least one *on* and one *off* spatially segregated subfield with either two subregions (S2) or three (S3). The LGN electrode was then positioned according to the map such that the LGN cell's receptive field overlapped with that of the simple cell. Finally, we targeted our retinal recording electrode via a rotating X-Y-Z stage and a rotating microelectrode carrier. We required that the receptive fields of the retinal, geniculate, and cortical units were at a similar eccentricity. In most experiments, small electrolytic lesions were made throughout the cortical penetration, and subsequent histology always verified that our simple cell recordings were confined to cortical layer 4 (the primary recipient zone of geniculate input).

Quantitative characterization of receptive fields was achieved with visual stimuli generated with an AT-Vista graphics card (Truevision, Indianapolis, IN). Stimuli were displayed on a 15 inch Nokia Multigraph 447× RGB monitor at a distance of 114 cm, with a frame (refresh) rate of 128 Hz and mean luminance of 90 cd/m^2. The monitor was linearized over the range of contrasts we used. A binary spatio–temporal white noise stimulus was used to obtain spatio–temporal receptive field maps (e.g., Figure 2A), as described previously (Reid et al., 1997). Individual stimulus pixels were either 0.4° or 0.8° wide, and the stimulus was updated every ~16 or 32 ms. We used the receptive field maps and responses to stimuli at various spatial frequencies and orientations to set the optimal parameters for the stimulus used to assess trial-by-trial (or cycle-by-cycle) variability. We chose a 4 Hz drifting sinusoidal grating of 50% contrast, as this stimulus was effective in driving cortical simple cells, as well as both X and Y neurons in the retina and LGN. The orientation of the grating was matched to the optimal orientation of the simple cell. Because the receptive field eccentricity of retinal, thalamic, and cortical cells was similar, responses at all three levels were typically strongly modulated by the same spatial frequency of the grating. The stimulus extended well beyond the classical receptive fields of all recorded neurons. Between 800 and 10,000 cycles of the grating stimulus were presented for each recording.

Our experiments required intraocular, high signal-to-noise recordings from single RGCs for extended periods (30–90 min). This was made possible by using the narrow diameter high impedance Ainsworth recording electrode, a headstage amplifier, and a stable electrode carrier. LGN electrodes were advanced with a Kopf 650 hydraulic microdrive (David Kopf Instruments, Tujunga, CA). Cortical electrodes were advanced with an MP 285 optically encoded stepper motorized micromanipulator (Sutter, Novato, CA).

Data Collection

All spike times and waveforms were recorded at 0.1 ms resolution and stored on the hard drive of a PC running Discovery data collection software (Datawave Technologies, Longmont, CO). All data were reanalyzed offline to confirm single unit isolation via waveform analysis, cluster cutting, and the presence of an absolute refractory period in the autocorrelogram or interspike interval histogram.

Second units on a single electrode were never discriminated in any of our retinal recordings, as they were nonexistent or too close to background noise. For our LGN cells, in only 2 of 17 cases was a second unit discriminated on a single electrode. For our cortical recordings, only 2 of 20 cells were second units from a single electrode. We only used second units that fired out of phase with the primary unit because the receptive fields were of opposite sign (*off* versus *on*) or completely spatially offset. Thus, when we resolved two well-isolated units from a single electrode, the recording was free of contamination by spikes that could have otherwise fired in synchrony.

Numerical Analysis

Fano Factor

We measured trial-by-trial variability by the FF, which is defined as the variance of the spike count divided by the mean:

$$FF = \frac{\sigma^2}{\mu}.$$

In all cases, we analyzed data from a single continuous 200 s presentation of a drifting grating, beginning with the response to the first cycle of the stimulus. For FF values given in Figures 2C and 3, the spike count was taken as the number of spikes in each stimulus cycle (250 ms) for the 800 cycles. When FF was analyzed as a function of time (t) in the stimulus cycle (Figures 4–6), the spike trains were divided into 200 nonoverlapping "repeats" of four stimulus cycles (1 s) each. This allowed us to consider counting windows of up to 1 s. We then counted the number of spikes per repeat in a sliding counting window of width T, evaluated at times t separated by 1 ms. Thus, the FF was a function of the counting window T, as well as the time in the repeat, t. A Poisson process has the property that FF(T,t) = 1 for any counting window T at all times t, regardless of the fact that the firing rate is varying with time within each trial. We emphasize that any given calculation of FF was based on samples taken from the same phase in the stimulus cycle (same epoch in PSTH), as opposed to samples taken from sequential windows of different phases (Vannucci and Teich, 1978; Teich et al., 1996).

We also calculated variability by an alternative measure, the Allan Factor (AF) (Thurner et al., 1997). The AF is similar to the FF except that instead of computing variability from the squared difference between each individual trial and the mean over all trials, we compute it from the squared difference between the number of spikes, N, in each individual trial (i) and the previous trial (i − 1):

$$AF = \frac{\langle (N_i - N_{i-1})^2 \rangle}{2\mu}.$$

The factor of 2 arises because the average squared difference of two samples is equal to twice the variance for a Poisson process. The AF effectively compares each trial with a temporally local mean count, so slow drifts in the mean do not affect the measure. The AF produced the same results as the FF for the range of counting window sizes we used (up to 1 s), indicating that the variability as measured by the FF was not significantly affected by drifts in firing rate (data not shown).

Model Spike Trains

Our data had lower variability than a time-varying Poisson process, for which FF = 1 in any counting window. To account for the reliability of our spike trains, we considered models with absolute and

relatively refractory periods, computed as described by Berry and Meister (1998). Briefly, the model spike train was generated from an underlying Poisson process with a time-varying rate called the "free firing rate." However, the probability of firing a spike at any instant was modified by recent spiking activity in that trial. In the case of the absolute refractory period models, the probability of firing is set to 0 for a specific length of time after each spike. We estimated each cell's absolute refractory period as the minimum interval between spikes in the entire recording period. Since we are confident that no spikes in our record could be from other cells, the true absolute refractory period might be shorter but cannot be longer than this estimate.

In the case of the relative refractory period models, we estimated the cell's relative refractory period from the interspike interval distribution. We fit an exponential to the part of the interspike interval distribution that showed exponential behavior, typically between $\sim$10 and $\sim$20 ms. We then estimated the recovery of spiking after an action potential by comparing the observed frequency of shorter intervals with that predicted from the exponential fit. The resulting recovery function, w(t), has an absolute refractory period and a longer period of reduced firing probability. This method makes the approximation that short intervals occur during a period of constant firing rate. Although this was not strictly true of our data, the approximation performed rather well under similar conditions in accounting for neural variability in the retina (Berry and Meister, 1998), as we also found for most of our data. The exception was bursting LGN cells, for which short intervals occurred in two distinct regimes: within bursts and between single spikes during epochs of high firing rate. For these cells, we had to use the interval distribution from only the nonburst response to obtain a good fit. For both refractory period models, we used the empirical procedure of Berry and Meister (1998) to obtain the free firing rate, q(t), for the underlying Poisson process. This is the rate that, after the effects of refractoriness, will produce the same time-varying firing rate as the neuron, r(t).

In addition to refractory models, we considered another variation on a Poisson model. As a benchmark against which to compare neural spiking statistics, the Poisson process is useful because it is described by a single parameter (rate) and is amenable to formal analysis. We also considered the more general set of gamma models, which are described by two parameters (rate and order). In a Poisson process, the distribution of interevent intervals is exponential. Each successive interval is drawn from this distribution independently, making it a "renewal" process. In a gamma process of order N, an event occurs every Nth such interval (a Poisson process is a gamma process of order 1). To generate an Nth order gamma process with the same time-varying rate as the cell, r(t), we generated a Poisson with a rate of N*r(t) and recorded a spike every Nth event. Each interval in the gamma process is the sum of N independent intervals, and therefore successive intervals of the gamma process are independent of one another. As the order increases, gamma processes become increasingly regular.

LGN Bursts

LGN cells exhibit a characteristic type of burst, with several sodium action potentials riding on the crest of a low-threshold calcium spike (Steriade and Llinás, 1988; McCormick and Feeser, 1990; reviewed by Sherman, 1996). These events can be recognized as a set of two to eight spikes separated by intervals of $<$4 ms, preceded by an interval of at least 100 ms without spiking activity (Lu et al., 1992). We used these interval criteria to identify bursts in our LGN responses.

Acknowledgments

We thank Christine Couture for expert technical assistance and Mal Teich for valuable discussions. Offline spike sorting and receptive field analysis software were developed by Sergey Yurgenson. We thank Tony Zador and John Reppas for helpful comments on an earlier version of the paper. This work was supported by National Institutes of Health grants R01-EY10115, P30-EY12196, and T32-NS07009 and the Brooks fund.

Received June 21, 2000; revised August 3, 2000.

References

Alonso, J.M., Usrey, W.M., and Reid, R.C. (1996). Precisely correlated firing in cells of the lateral geniculate nucleus. Nature *383*, 815–819.

Bair, W., and O'Keefe, L.P. (1998). The influence of fixational eye movements on the response of neurons in area MT of the macaque. Vis. Neurosci. *15*, 779–786.

Barberini, C.L., Horwitz, G.D., and Newsome, W.T. (2000). A comparison of spiking statistics in motion sensing neurons of flies and monkeys. In Computational, Neural and Ecological Constraints of Visual Motion Processing, J. Zeil and J.M. Zanker, eds. (NY: Springer-Verlag), in press.

Barlow, H.B., and Levick, W.R. (1969). Changes in the maintained discharge with adaptation level in the cat retina. J. Physiol. (Lond) *202*, 699–718.

Berry, M.J., Warland, D.K., and Meister, M. (1997). The structure and precision of retinal spike trains. Proc. Natl. Acad. Sci. USA *94*, 5411–5416.

Berry, M.J., II, and Meister, M. (1998). Refractoriness and neural precision. J. Neurosci. *18*, 2200–2211.

Buračas, G.T., Zador, A.M., DeWeese, M.R., and Albright, T.D. (1998). Efficient discrimination of temporal patterns by motion-sensitive neurons in primate visual cortex. Neuron *20*, 959–969.

Dean, A.F. (1981). The variability of discharge of simple cells in the cat striate cortex. Exp. Brain Res. *44*, 437–440.

deCharms, R.C., and Zador, A. (2000). Neural representation and the cortical code. Annu. Rev. Neurosci. *23*, 613–647.

de Ruyter van Steveninck, R.R., Lewen, G.D., Strong, S.P., Koberle, R., and Bialek, W. (1997). Reproducibility and variability in neural spike trains. Science *275*, 1805–1808.

Ferster, D. (1996). Is neural noise just a nuisance? Science *273*, 1812.

Frishman, L.J., and Levine, M.W. (1983). Statistics of the maintained discharge of cat retinal ganglion cells. J. Physiol. (Lond) *339*, 475–494.

Gazères, N., Borg-Graham, L.J., and Frégnac, Y. (1998). A phenomenological model of visually evoked spike trains in cat geniculate nonlagged X-cells. Vis. Neurosci. *15*, 1157–1174.

Geisler, W.S., and Albrecht, D.G. (1997). Visual cortex neurons in monkeys and cats: detection, discrimination, and identification. Vis. Neurosci. *14*, 897–919.

Gershon, E.D., Wiener, M.C., Latham, P.E., and Richmond, B.J. (1998). Coding strategies in monkey V1 and inferior temporal cortices. J. Neurophysiol. *79*, 1135–1144.

Guido, W., and Sherman, S. (1998). Response latencies of cells in the cat's lateral geniculate nucleus are less variable during burst than tonic firing. Vis. Neurosci. *15*, 231–237.

Gur, M., Beylin, A., and Snodderly, D.M. (1997). Response variability of neurons in primary visual cortex (V1) of alert monkeys. J. Neurosci. *17*, 2914–2920.

Hartveit, E., and Heggelund, P. (1994). Response variability of single cells in the dorsal lateral geniculate nucleus of the cat: comparison with retinal input and effect of brain stem stimulation. J. Neurophysiol. *72*, 1278–1289.

Heggelund, P., and Albus, K. (1978). Response variability and orientation discrimination of single cells in striate cortex of cat. Exp. Brain Res. *32*, 197–211.

Jahnsen, H., and Llinás, R. (1984). Ionic basis for the electroresponsiveness and oscillatory properties of guinea-pig thalamic neurones in vitro. J. Physiol. (Lond) *349*, 227–247.

Kara, P., and Friedlander, M.J. (1999). Arginine analogs modify signal detection by neurons in the visual cortex. J. Neurosci. *19*, 5528–5548.

Kisley, M.A., and Gerstein, G.L. (1999). Trial-to-trial variability and state-dependent modulation of auditory-evoked responses in cortex. J. Neurosci. *19*, 10451–10460.

Lankheet, M.J., Molenaar, J., and van de Grind, W.A. (1989). The

spike generating mechanism of cat retinal ganglion cells. Vision Res. *29*, 505–517.

Lee, C., Malpeli, J.G., Schwark, H.D., and Weyand, T.G. (1984). Cat medial interlaminar nucleus: retinotopy, relation to tapetum and implications for scotopic vision. J. Neurophysiol. *52*, 848–869.

Lee, D., Lee, C., and Malpeli, J.G. (1992). Acuity-sensitivity tradeoffs of X and Y cells in the cat lateral geniculate complex: role of the medial interlaminar nucleus in scotopic vision. J. Neurophysiol. *68*, 1235–1247.

Levine, M.W., Cleland, B.G., and Zimmerman, R.P. (1992). Variability of responses of cat retinal ganglion cells. Vis. Neurosci. *8*, 277–279.

Levine, M.W., Cleland, B.G., Mukherjee, P., and Kaplan, E. (1996). Tailoring of variability in the lateral geniculate nucleus of the cat. Biol. Cybern. *75*, 219–227.

Lu, S.M., Guido, W., and Sherman, S.M. (1992). Effects of membrane voltage on receptive field properties of lateral geniculate neurons in the cat: contributions of the low-threshold Ca^{2+} conductance. J. Neurophysiol. *68*, 2185–2198.

McAdams, C.J., and Maunsell, J.H. (1999). Effects of attention on the reliability of individual neurons in monkey visual cortex. Neuron *23*, 765–773.

McCormick, D.A., and Feeser, H.R. (1990). Functional implications of burst firing and single spike activity in lateral geniculate relay neurons. Neuroscience *39*, 103–113.

Merrill, E.G., and Ainsworth, A. (1972). Glass-coated platinum-plated tungsten electrodes. Med. Biol. Eng. *10*, 662–672.

Oram, M.W., Wiener, M.C., Lestienne, R., and Richmond, B.J. (1999). Stochastic nature of precisely timed spike patterns in visual system neural responses. J. Neurophysiol. *81*, 3021–3033.

Pettigrew, J.D., Cooper, M.L., and Blasdel, G.G. (1979). Improved use of tapetal reflection for eye-position monitoring. Invest. Ophthalmol. Vis. Sci. *18*, 490–495.

Reich, D.S., Victor, J.D., Knight, B.W., Ozaki, T., and Kaplan, E. (1997). Response variability and timing precision of neuronal spike trains in vivo. J. Neurophysiol. *77*, 2836–2841.

Reid, R.C., and Alonso, J.M. (1995). Specificity of monosynaptic connections from thalamus to visual cortex. Nature *378*, 281–284.

Reid, R.C., Victor, J.D., and Shapley, R.M. (1997). The use of m-sequences in the analysis of visual neurons: linear receptive field properties. Vis. Neurosci. *14*, 1015–1027.

Reinagel, P., and Reid, R.C. (2000). Temporal coding of visual information in the thalamus. J. Neurosci. *20*, 5392–5400.

Reinagel, P., Godwin, D., Sherman, S.M., and Koch, C. (1999). Encoding of visual information by LGN bursts. J. Neurophysiol. *81*, 2558–2569.

Rieke, F., Warland, D., de Ruyter van Steveninck, R., and Bialek, W. (1997). Spikes (Cambridge, MA: MIT Press).

Rodieck, R.W. (1967). Maintained activity of cat retinal ganglion cells. J. Neurophysiol. *30*, 1043–1071.

Sanderson, K.J. (1971a). The projection of the visual field to the lateral geniculate and medial interlaminar nuclei in the cat. J. Comp. Neurol. *143*, 101–118.

Sanderson, K.J. (1971b). Visual field projection columns and magnification factors in the lateral geniculate nucleus of the cat. Exp. Brain Res. *13*, 159–177.

Sestokas, A.K., and Lehmkuhle, S. (1988). Response variability of X- and Y-cells in the dorsal lateral geniculate nucleus of the cat. J. Neurophysiol. *59*, 317–325.

Shadlen, M.N., and Newsome, W.T. (1998). The variable discharge of cortical neurons: implications for connectivity, computation, and information coding. J. Neurosci. *18*, 3870–3896.

Sherman, S.M. (1996). Dual response modes in lateral geniculate neurons: mechanisms and functions. Vis. Neurosci. *13*, 205–213.

Skottun, B.C., Bradley, A., Sclar, G., Ohzawa, I., and Freeman, R.D. (1987). The effects of contrast on visual orientation and spatial frequency discrimination: a comparison of single cells and behavior. J. Neurophysiol. *57*, 773–786.

Snowden, R.J., Treue, S., and Andersen, R.A. (1992). The response of neurons in areas V1 and MT of the alert rhesus monkey to moving random dot patterns. Exp. Brain Res. *88*, 389–400.

Softky, W.R., and Koch, C. (1993). The highly irregular firing of cortical cells is inconsistent with temporal integration of random EPSPs. J. Neurosci. *13*, 334–350.

Stein, R.B. (1965). A theoretical analysis of neuronal variability. Biophys. J. *5*, 173–194.

Steriade, M., and Llinás, R.R. (1988). The functional states of the thalamus and the associated neuronal interplay. Physiol. Rev. *68*, 649–742.

Stratford, K.J., Tarczy-Hornoch, K., Martin, K.A.C., Bannister, N.J., and Jack, J.J.B. (1996). Excitatory synaptic inputs to spiny stellate cells in cat visual cortex. Nature *382*, 258–261.

Swindale, N.V., and Mitchell, D.E. (1994). Comparison of receptive field properties of neurons in area 17 of normal and bilaterally amblyopic cats. Exp. Brain Res. *99*, 399–410.

Tanaka, K. (1983). Cross-correlation analysis of geniculostriate neuronal relationships in cats. J. Neurophysiol. *49*, 1303–1318.

Teich, M.C., and Diament, P. (1980). Relative refractoriness in visual information processing. Biol. Cybern. *38*, 187–191.

Teich, M.C., Matin, L., and Cantor, B.I. (1978). Refractoriness in the maintained discharge of the cat's retinal ganglion cell. J. Opt. Soc. Am. *68*, 386–402.

Teich, M.C., Turcott, R.G., and Siegel, R.M. (1996). Temporal correlation in cat striate-cortex neural spike trains. IEEE Eng. Med. Biol. Mag. *15*, 79–87.

Thurner, S., Lowen, S.B., Feurstein, M.C., Heneghan, C., Feichtinger, H.G., and Teich, M.C. (1997). Analysis, synthesis, and estimation of fractal-rate stochastic point processes. Fractals *5*, 565–595.

Tolhurst, D.J., Movshon, J.A., and Dean, A.F. (1983). The statistical reliability of signals in single neurons in cat and monkey visual cortex. Vision Res. *23*, 775–785.

Vannucci, G., and Teich, M.C. (1978). Effects of rate variation on the counting statistics of dead-time-modified Poisson processes. Opt. Commun. *25*, 267–272.

Vogels, R., Spileers, W., and Orban, G.A. (1989). The response variability of striate cortical neurons in the behaving monkey. Exp. Brain Res. *77*, 432–436.